

Accurate Time Domain Zero Voltage Switching Analysis of a Dual Active Bridge with Triple Phase Shift

Fabian Sommer, Nikolas Menger, Tobias Merz, Marc Hiller
Karlsruhe Institute of Technology (KIT)
Elektrotechnisches Institut (ETI) - Power Electronic Systems
Kaiserstraße 12
Karlsruhe, Germany
Phone: +49 721 608-42477
Email: fabian.sommer@kit.edu
URL: <https://www.eti.kit.edu>

Keywords

«Zero - voltage switching», «Dual Active Bridge (DAB)», «DC-DC converter», «Solid-State Transformer», «soft switching»

Abstract

In this paper an accurate capacitance time domain model (CTD) of the Zero Voltage Switching (ZVS) behaviour of a Dual Active Bridge considering deadtime, MOSFET Drain-Source capacitances and transformer stray inductances is presented. Building upon this a DAB model considering voltage-time errors caused by resonant commutation for Single Phase Shift (SPS) and Triple Phase Shift (TPS) is derived. Additionally a formula to calculate the optimal deadtime according to the CTD is proposed. Measurements at different operation points validate the consistency of the resonant commutation model and the voltage-time error model for the DAB.

Introduction

The Dual Active Bridge (DAB) shown in Fig. 1(a) has various advantages including soft switching capability, low passive component effort and galvanic isolation. Because of high switching frequencies and high efficiency requirements, soft switching is necessary. There are two soft switching techniques which can be used in DAB applications. The first one is Zero Current Switching (ZCS) where the switching occurs at zero (or close to zero) current to avoid switching losses. Since the behaviour at ZCS is easy to model and describe, it will not be further investigated. The second soft switching technique is the resonant Zero Voltage Switching (ZVS) which drastically reduces the turn-on losses of the MOSFETs. There are multiple methods for the modeling ZVS behaviour. The easiest and widely used method is by checking solely the MOSFET's current direction. It is assumed that a negative current leads to a ZVS turn on [1]. However, this method does not consider parasitic capacitances during the commutation. Another common method which includes the parasitic capacitance is done by comparing the overall energy inside the output capacitance C_{eq} of the MOSFETs $E_C = 0.5C_{eq}U_{DS}^2$ and the stored energy inside the stray inductance $E_\sigma = 0.5L_\sigma I_{L_\sigma}^2$ of the transformer and parasitics of the converter. This method is known as current-dependent charge-based (CDCB) ZVS modelling [2]. If the energy E_σ is higher or equal to E_C , ZVS is possible. If the energy E_σ is below E_C , hard switching occurs. Since this boundary ignores deadtime, partial soft switching behaviour and the waveform for commutation a more accurate model is necessary to predict the resonant commutation reliably. In [3] a more accurate charged based model is presented. Another possible model is presented in [4] and calculates a time domain model for the resonant commutation for Single Phase Shift (SPS) modulation.

The new developed method will further investigate a capacitance time domain based model (CTD) for a generalized triple phase shift (TPS) modulation. Since the deadtime and the resonant commutation results in significant voltage error and therefore a power transfer error the influence of commutation can not be neglected [5]. To evaluate this phenomenon a voltage error model is derived from the CTD. Both analytical models are compared with measurement results to evaluate the accuracy. With these results it will be possible to accurately predict ZVS boundary and behavior, including partial soft switching, as well as the calculation of the output voltage and the AC current during commutation, enabling the compensation of offset voltages.

Equivalent circuit diagram of the resonant switching circuit

In this section the work flow to derive the accurate soft switching equivalent circuit is presented for SPS and TPS modulation. In order to calculate the resonant commutation process of the DAB, an accurate model is required. Figure 1 shows the current paths for different resonant commutations within SPS and TPS of a DAB. There are two different cases of resonant commutation to be discussed all other switching events are a combination of these two:

- Case 1: Switching event in one half bridge (Fig. 1b)
- Case 2: Switching event in one full bridge (Fig. 1c)

Additionally a combination of both switching events is possible as well as a switching event on the secondary side within the deadtime of the primary side as shown in Fig. 1d. For all further calculations and considerations, it is assumed that no other switching event occurs within the deadtime and for simplicity the transformer ratio is assumed to be 1.

In the example shown in Fig. 1a and Fig. 1b T1 and T4 are turned off and T2 and T3 are turned on with an initial positive current through T1/T4. Both current paths are highlighted in red and green, respectively. It is important to assume that for this simple example, the secondary side of the DAB has no switching events and therefore, it can be modeled as a constant voltage source (v_{AC2}) since it provides a constant voltage at the secondary winding of the transformer. This assumption only holds if $C_{DC2} \gg C_{eq}$. The resulting equivalent circuit diagram is shown in Fig. 1c. It represents a resonant circuit between the stray inductance and the output capacitances of the MOSFETs and the DC-Link capacitance. The resulting equivalent capacitance C_{eq} for case 1 is calculated in (1a). For $C_{DC2} \gg C_{T1-T4}$ and $C_{T1} = C_{T2} = C_{T3} = C_{T4} = C_T$ the simplification also shown in (1a) can be used. Table I shows the equivalent capacitance for all possible switching events for the discussed simplifications. For all further investigations the voltage dependent drain source capacitance C_{DS} of the MOSFETs is assumed as voltage independent. This assumption is admissible because the largest gradient in capacitance is for the first 10VV and therefore the overall impact negligible since the total energy has a quadratic relationship with the the voltage. Additionally the serial and parallel network of capacitances reduces the influence of the voltage dependency.

$$C_{eq} = \frac{C_a \left(\frac{C_b C_{T1}}{C_b + C_{T1}} + \frac{C_c C_{T3}}{C_c + C_{T3}} \right)}{C_a + \frac{C_b C_{T1}}{C_b + C_{T1}} + \frac{C_c C_{T3}}{C_c + C_{T3}}} \approx C_T \quad (1a)$$

$$C_a = \frac{C_{T2} C_{DC1} + C_{T2} C_{T4} + C_{T4} C_{DC1}}{C_{DC1}} \quad (1b)$$

$$C_b = \frac{C_{T2} C_{DC1} + C_{T2} C_{T4} + C_{T4} C_{DC1}}{C_{T4}} \quad (1c)$$

$$C_c = \frac{C_{T2} C_{DC1} + C_{T2} C_{T4} + C_{T4} C_{DC1}}{C_{T2}} \quad (1d)$$

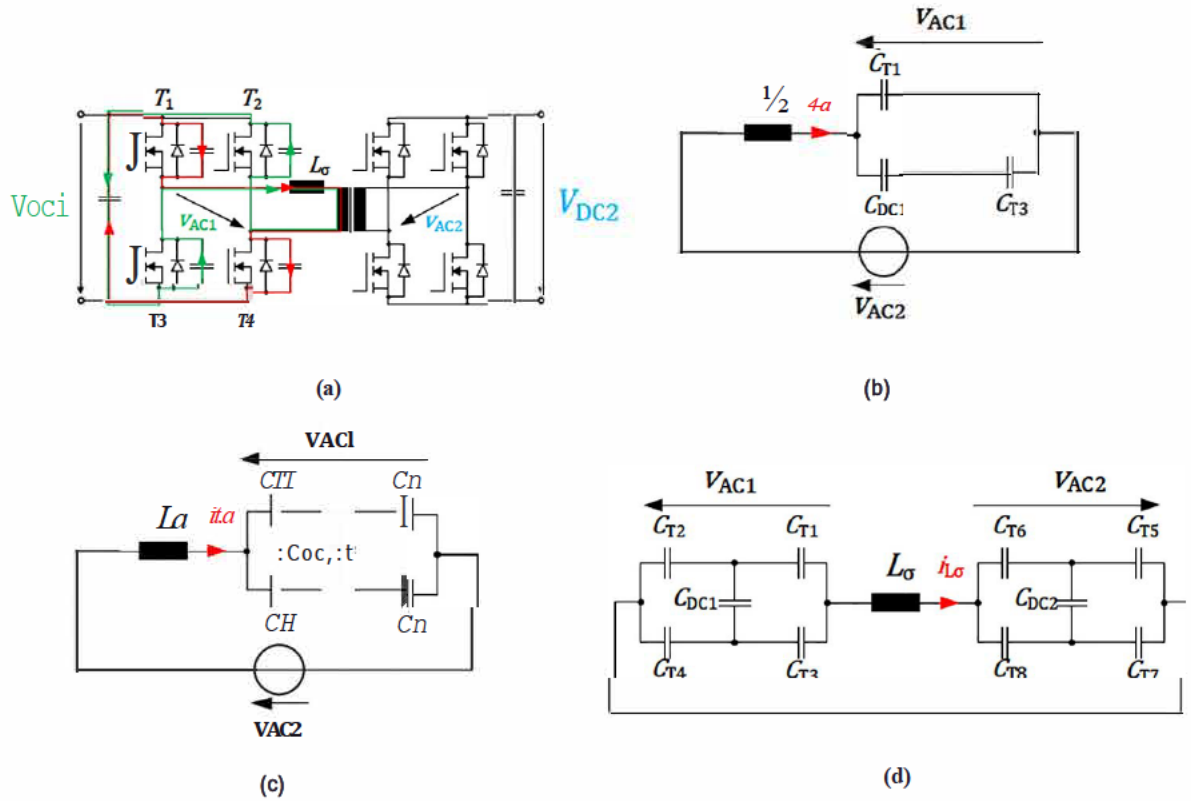


Fig. 1: (a) Current path for resonant commutation (SPS) (b) equivalent circuit diagram of commutation (SPS) (c) commutation in one half bridge (d) commutation in all four half bridges at the same time

Table I: Equivalent capacitances for all switching events with equal Cos and $\text{Coc1} \gg \text{Cos}$

	one half bridge	two half bridges	three half bridges	four half bridges
C_{eq}	$2 \cdot C_T$	C_T	$\frac{2 \cdot C_T}{3}$	$\frac{C_T}{2}$

Table II shows the starting conditions V_0 and i_0 as well as the final condition for the parasitic capacitances and inductance within the commutation circuit when ZVS is fully achieved. If ZVS is only partially achieved, the end value will be between the given values in Table II.

Table II: starting and final condition of the parasitic capacitances and inductance for case 2

	starting condition	final condition for ZVS
$C1$	$V_0 = 0$	V_{oci}
$C3$	$V_0 = V_{oci}$	0
$C2$	$V_0 = V_{oci}$	0
$C4$	$V_0 = 0$	V_{oci}
Coc1	$V_0 = V_{oci}$	V_{oci}
L_a	$i_0 = i_{L\sigma}$	

Analysis in the complex frequency domain

With the obtained model the analysis in the complex frequency domain is possible. The resulting current through the inductor is calculated by applying Kirchhoff's Law on the equivalent circuit diagram in Fig. 1(b) and using the equation (1a). The result is given in (2) for the complex frequency domain and in

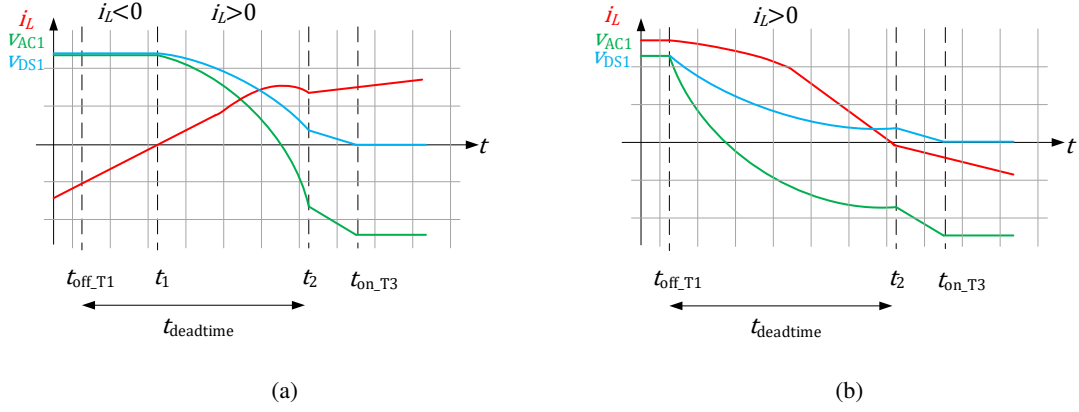


Fig. 2: Theoretical waveforms for a resonant commutation process (partial ZVS) (a) with negative starting current (b) with positive starting current

(3) for the time domain. The inductor current $i_{L,\sigma}$ depends on the starting conditions from Table II, the voltage applied by the secondary side and the parasitic components on the primary side at the same time.

$$i_{L,\sigma}(s) = \frac{L_\sigma i_0 + \frac{V_0}{s} - \frac{v_{AC2}}{s \cdot n}}{L_\sigma s + \frac{1}{C_{eq} \cdot s}} = \frac{s L_\sigma i_0 + V_0 - \frac{v_{AC2}}{n}}{L_\sigma s^2 + \frac{1}{C_{eq}}} \quad (2)$$

$$i_{L,\sigma}(t) = i_0 \cdot \cos\left(\frac{t}{\sqrt{L_\sigma C_{eq}}}\right) + \sqrt{\frac{C_{eq}}{L_\sigma}} (V_0 - v_{AC2}) \cdot \sin\left(\frac{t}{\sqrt{L_\sigma C_{eq}}}\right) \quad (3)$$

$$i_{C,T1}(t) = i_{L,\sigma}(t) \cdot \frac{C_{T3}}{C_{T3} + C_{T1}} \quad (4)$$

By integrating (3) in the time frame of the deadtime, the voltage at the H-bridge output v_{AC1} can be determined and is shown in (5). By solving the equation in (5) the output voltage can be calculated with (6). From this it can be seen that the amplitude of the resonant oscillation depends on the stray inductance, the equivalent capacitance, the switching current and the output voltages of both H-bridges and determines if full ZVS is possible or not. The resulting resonance frequency and therefore also the voltage steepness at the output depends mainly on the time constant $\sqrt{L_\sigma C_{eq}}$ and determines the minimal deadtime necessary for ZVS or partial ZVS. To calculate the voltage v_{DS} at every MOSFET the current through the associated capacitances can be calculated according to (4) and integrated similar as shown in (5).

$$v_{AC1}(t) = -\frac{1}{C_{eq}} \cdot \int_0^t i_{L,\sigma} dt + V_{DC1} \quad (5)$$

$$v_{AC1}(t) = -\sqrt{\frac{L_\sigma}{C_{eq}}} \left(i_0 \sin\left(\frac{t}{\sqrt{L_\sigma C_{eq}}}\right) \right) + (V_0 - v_{AC2}) \left(\cos\left(\frac{t}{\sqrt{L_\sigma C_{eq}}}\right) - 1 \right) + V_{DC1} \quad (6)$$

Figure 2 shows the theoretical waveforms of the AC current $i_{L,\sigma}$, the drain source voltage v_{DS1} and the H-Bridge output voltage v_{AC1} for a resonant commutation with partial ZVS. There are three possible

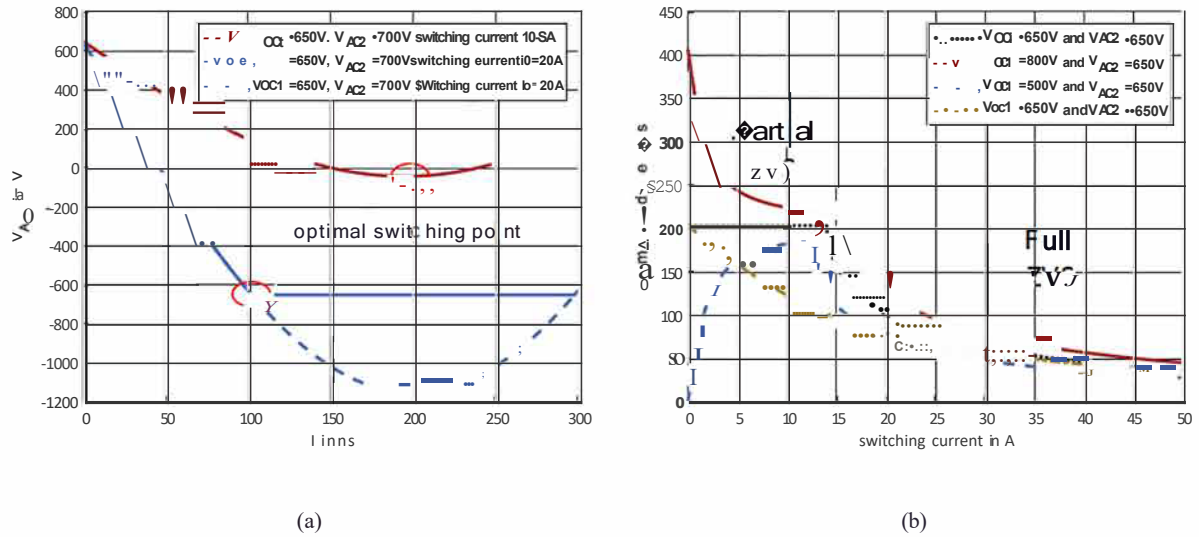


Fig. 3: (a) Optimal deadtime with respect to the switching current for different voltages (b) Optimal switching points for different switching currents

cases. The first one is a negative inductor current during the whole deadtime which results in a resonant commutation because the anti parallel diode of the turned off MOSFET can not conduct the current. In this case the following applies to the voltages: $v_{os1} = v_{AC1} = V_{oc1}$ for $0 < t < t_2$ ($t_1 = t_2$), when MOSFET T3 is turned on. After that, full switching losses occur and no 'ZVS is achieved. The second possible case is when a negative starting current occurs but the current direction is changing within the deadtime. This is depicted in Fig. 2a. When the current changes its sign at $t = t_1$ the capacitances can be charged and v_{OC1} and v_{AC1} are decreased. At $t = t_2$ (after the deadtime) T3 is turned on and partial or full 'ZVS is possible. The third case is a positive current at the start of the commutation ($t_1 = t_{off}, T1$). In this case the voltages are decreased until the end of the deadtime is reached at $t = t_2$ and partial or full 'ZVS occurs (Fig. 2b).

The Optimal Deadtime

As discussed in the previous chapter, the resonant commutation and soft switching only occurs within in the deadtime of every half bridge. Hence the deadtime is an important parameter to ensure minimal switching losses and to achieve partial or full 'ZVS. In equation (6) an analytical expression to calculate the AC voltage v_{ac} in case of resonant switching is presented. The resulting voltage is shown for two different operating points in Fig. 3a. In case of the red curve only partial 'ZVS is achieved because the energy stored in the magnetic field of the stray inductance is not sufficient to charge the equivalent capacitance C_{eq} . For the blue curve full 'ZVS can be achieved. For this operating point the resonant oscillation reaches the negative DC link voltage. After that the diodes of the MOSFETs suppress further oscillations and the AC voltage v_{AC1} remains at $v_{AC1} = -V_{oc1}$. To minimize switching losses the turn on after the deadtime should be at the minimal possible voltage (marked with red circle). Depending on whether complete or only partial 'ZVS is possible the two marked minimal switching points from Fig. 3a must be calculated. In the case of full 'ZVS the minimal deadtime $T_{on12,opt,fullZVS}$ is calculated by (7a) for case 1 and (7b) for case 2 and corresponds to the blue curve of Fig. 3a. If the deadtime is longer than these calculated values, full 'ZVS is achieved. For partial ZVS the optimal deadtime $T_{on12,opt,parZVS}$ is calculated by (8) and provides the first minimum of the voltage oscillations as show at the red curve in Fig. 3b. Since before and after that calculated time the switching voltage is increasing, the deadtime should be accurate to that equation for minimal switching losses.

$$T_{DT1,opt,fullZVS} = \pm\sqrt{b} \cdot \arccos \left(\frac{\pm\sqrt{a^2 i_0^4 - 4 \cdot a i_0^2 \cdot V_0 \cdot v_{ac2} - V_0^2 + v_{ac2}^2}}{a \cdot i_0^2 - V_0 \cdot v_{ac2} + v_{ac2}^2 + V_0^2} \right) \quad (7a)$$

$$T_{DT2,opt,fullZVS} = \pm\sqrt{b} \cdot \arccos \left(\frac{\pm\sqrt{a^2 i_0^4 - 2 \cdot a i_0^2 \cdot V_0 \cdot v_{ac2} + a \cdot i_0^2 \cdot V_0^2 - V_0 \cdot v_{ac2} + v_{ac2}^2}}{a \cdot i_0^2 - 2 \cdot V_0 \cdot v_{ac2} + v_{ac2}^2 + V_0^2} \right) \quad (7b)$$

$$T_{DT,opt,parZVS} = \sqrt{b}(\pi + \arctan \left(\frac{i_0 \sqrt{a}}{V_0 - v_{ac}} \right)) \quad (8)$$

$$\text{with } a = \frac{L_\sigma}{C_{eq}} \text{ and } b = L_\sigma C_{eq}$$

The resulting optimal deadtime for different voltages and switching currents is shown in Fig. 3b. Depending on the switching current i_0 and the voltage on the secondary side v_{AC2} , full or only partial ZVS can be achieved, as marked in the plot. For low currents full ZVS can only be achieved if the voltage on the secondary side is negative (brown plot), at higher currents full ZVS is always possible. As described earlier for partial ZVS the graphs in Fig. 3b shows the optimal deadtime that should be met and for full ZVS the minimal necessary deadtime for full ZVS but higher deadtimes are possible too. This model can help to improve the efficiency especially under light load situations by reducing switching losses when full ZVS is not possible anymore.

Voltage Error Model

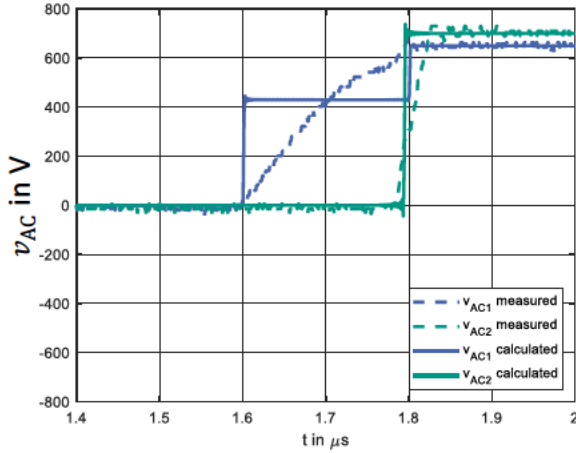
Since most state of the art DAB models consider $t_{deadtime} \ll t_{phaseshift}$, voltage errors caused by commutation are negligible. Since for low power transfer and low stray inductances the deadtime has an influence that cannot be neglected. Depending on the resonant switching the transmitted power can vary greatly from the theoretical model. In addition, the circular currents caused by modulation and commutation can increase strongly due to the voltage error and the switching currents can vary from the theoretical optimal points. Both can lead to increased losses if the commutation is not taken into account. To consider this error for the DAB, a voltage error model is developed. The common approach is done by evaluating the current sign at the start of the switching event and to delay the voltage switching if the current is negative through the the MOSFET which is turned off. This deadtime voltage error model is only accurate if no resonant switching occurs and the current sign is not changing within a switching event.

To improve the modeling of the voltage error, equation (6) can be used to calculate the AC voltage in case of resonant commutation. By integrating the AC voltage over the whole commutation process the equivalent AC voltage can be calculated. To reduce computational effort, the voltage error is approximated as a constant voltage for the whole deadtime. The resulting amplitude of the voltage step equivalent to the voltage error for the deadtime is given in equation (9) and (6) with $v_{AC1,ideal}$ as the AC voltage with infinity fast commutation.

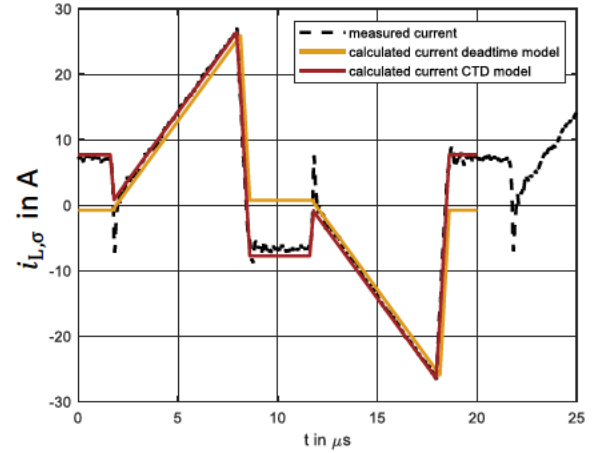
$$v_{AC1,eq} = v_{AC1,ideal} - \int_{t_0}^{t_{deadtime}} v_{AC1} dt \quad (9)$$

Validation of the CTD Model with Measurement Results

To validate the calculations, measurements on a DAB are done. The parameters of the measurement setup are shown in Table III and the used DAB is depicted in Fig. 5. The results are shown for different



(a)



(b)

Fig. 4: Measurement results for $V_{DC1} = 650V$ and $V_{DC1} = 700V$ (a) AC voltages for one commutation compared with calculated voltages considering voltage error (b) AC current compared to deadtime method and CTD method

Parameter	setup value
C_{DS}	0.6 nF
C_{DC}	60 μ F
$V_{DC,max}$	800V
$t_{deadtime}$	200 ns
L_{σ}	12 μ H
$P_{out,max}$	35 kW
n	1
f_{sw}	50 kHz

Table III: Parameters of the DAB

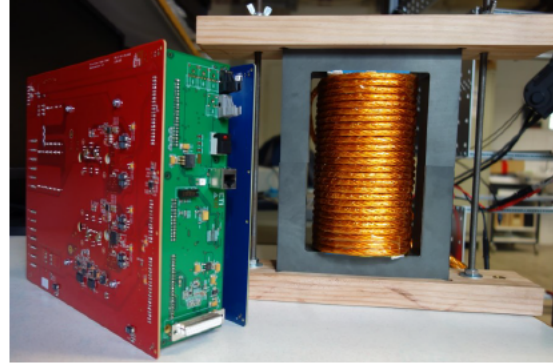


Fig. 5: Dual Active Bridge with Transformer

operation points in Fig. 6. The dotted lines are the measured AC current and the output voltage v_{AC1} . The solid lines represent the calculated waveforms for the resonant commutation according to (3) and (6). Since the model only considers the resonant commutation and no hard switching events, the calculated values are only available for the deadtime of $t_{deadtime} = 200$ ns. To evaluate the model for all cases discussed, different operation points are depicted. Figure 6a and Fig. 6b shows two partial ZVS events, in Fig. 6c is a partial ZVS event with a negative starting current is depicted and in Fig. 6d is a full ZVS event shown. For all cases the calculated waveforms match the measured curves within the deadtime.

To evaluate both proposed voltage error models the ac voltages v_{AC1} , v_{AC2} and the ac current $i_{L,\sigma}$ are compared with measurements. The results are shown in Fig. 4. The dotted lines are the measured values and the solid lines are the calculated waveforms. By comparing the currents for the deadtime model and the CTD model it can be seen that CTD model corresponds very accurately to the measurement whereas the deadtime model shows clear deviations. Remaining errors for the CTD model are caused by parasitic capacitances of the transformer and the difficulty of parameterising the system as well as the simplifications. Due to the small leakage inductance of the transformer, voltage errors can be detected especially in the AC current $i_{L,\sigma}$. Since the deviations are very small, the model can accurately predict the

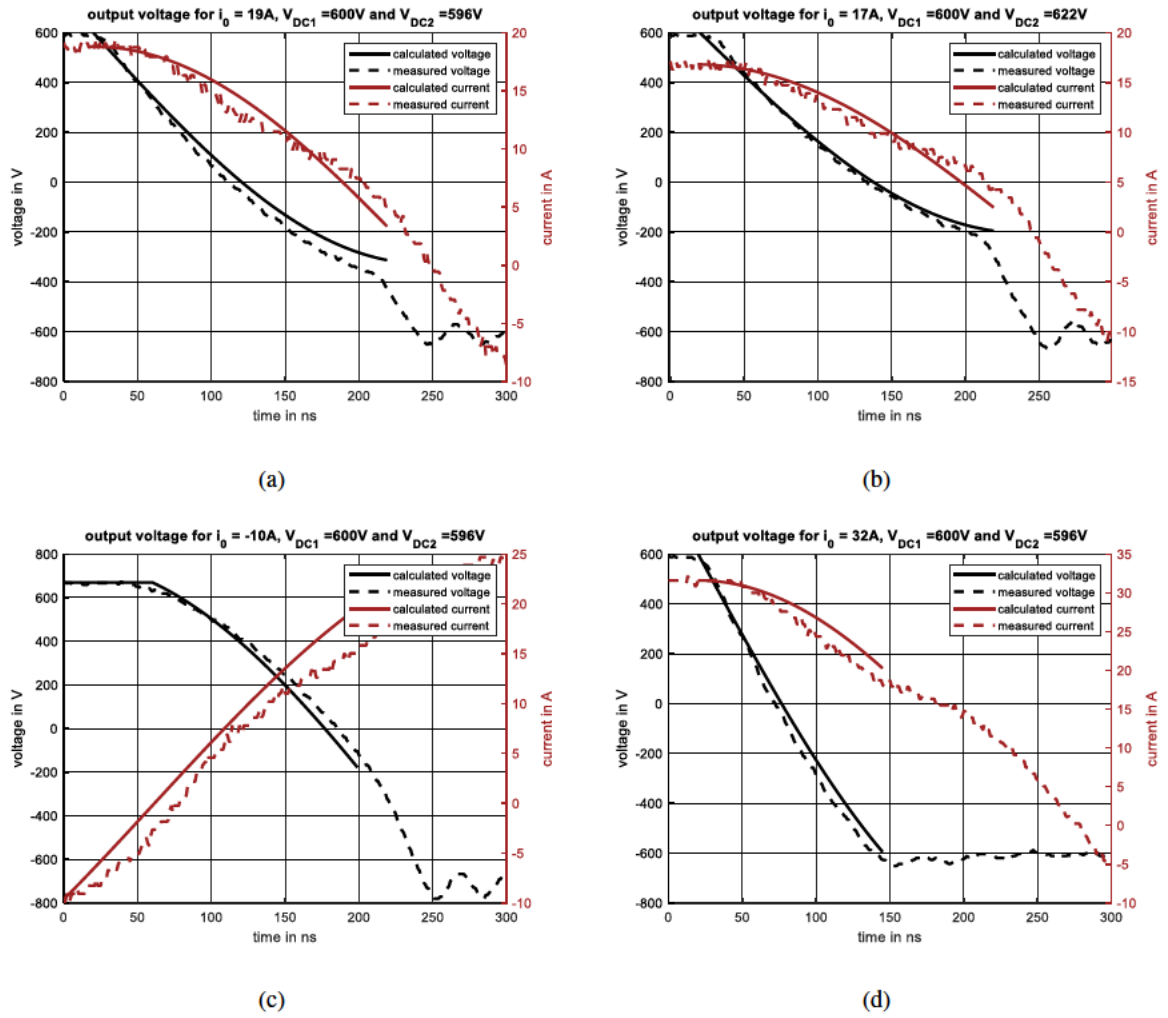


Fig. 6: Comparison of measured and calculated waveforms of the AC voltage v_{AC1} and the AC current $i_{L,\sigma}$ for partial and full ZVS for T2. (a) partial ZVS (b) partial ZVS in boost mode (c) partial ZVS for negative starting current (d) full ZVS

behaviour of the DAB even with high impact of the commutation. To compare the voltages Fig. 4b shows the measured voltages and the calculated voltages according to the CTD model. It can be observed that the voltage time area for the commutation is equal. In the final step the transmitted power is compared for this operation point and is shown in Table IV. Using the CTD model the power error can be significantly reduced.

Table IV: Trasmitted power for the different voltage error methods

	deadtime model	CTD model	measurement
P_{mean}	5660W	5804W	5823W

Conclusion

This paper presents a novel capacitance time domain Zero Voltage Switching model for a Dual Active Bridge with Triple Phase Shift modulation. The model is acquired by using an equivalent circuit diagram for the resonant commutation within the deadtime. Different ZVS cases are discussed, analysed and compared with measurements acquired on a real measurement setup. The results are matching with the measurements. Based on the acquired model the optimal deadtime can be calculated and an accurate

voltage error model is derived. Measurements with a hardware setup can also confirm these models.

References

- [1] S. S. Shah, V. M. Iyer and S. Bhattacharya, "Exact Solution of ZVS Boundaries and AC-Port Currents in Dual Active Bridge Type DC-DC Converters," in *IEEE Transactions on Power Electronics*, vol. 34, no. 6, pp. 5043-5047, June 2019
- [2] Y. Yan, H. Gui and H. Bai, "Complete ZVS Analysis in Dual Active Bridge," in *IEEE Transactions on Power Electronics*, vol. 36, no. 2, pp. 1247-1252, Feb. 2021
- [3] J. Everts, F. Krismer, J. Van den Keybus, J. Driesen and J. W. Kolar, "Charge-based ZVS soft switching analysis of a single-stage dual active bridge AC-DC converter," 2013 *IEEE Energy Conversion Congress and Exposition*, Denver, CO, 2013
- [4] X. Fei, Z. Feng, N. PuQi and W. Xuhui, "Analyzing ZVS Soft Switching Using Single Phase Shift Control Strategy of Dual Active Bridge Isolated DC-DC Converters," 2018 21st *International Conference on Electrical Machines and Systems (ICEMS)*, Jeju, 2018, pp. 2378-2381
- [5] J. Itoh, K. Kawauchi and H. Watanabe, "Non-linear Dead-time Error Compensation Method of Dual Active Bridge DC-DC Converter for Variable DC-bus Voltage," 2018 *International Conference on Smart Grid (icSmartGrid)*, 2018, pp. 208-213